Published in final edited form as:
Nat Neurosci. 2010 July ; 13(7): 861–868. doi:10.1038/nn.2581.

Specific roles for DEG/ENaC and TRP channels in touch and thermosensation in *C. elegans* nociceptors

Marios Chatzigeorgiou[1], **Sungjae Yoo**[6], **Joseph D. Watson**[4], **Wei-Hsiang Lee**[3], **W. Clay Spencer**[4], **Katie S. Kindt**[2], **Sun Wook Hwang**[6], **David M. Miller III**[4], **Millet Treinin**[5], **Monica Driscoll**[3], and **William R. Schafer**[1,2]

[1]Cell Biology Division, MRC Laboratory of Molecular Biology, Hills Road, Cambridge UK

[2]Division of Biology, University of California, San Diego, La Jolla CA USA

[3]Department of Molecular Biology and Biochemistry, Nelson Biological Laboratories, Rutgers, The State University of New Jersey, Piscataway, NJ USA

[4]Department of Cell and Developmental Biology, Vanderbilt University, Nashville, TN USA

[5]Department of Medical Neurobiology, IMRIC, Hebrew University-Hadassah Medical School, Jerusalem, Israel

[6]Korea University Graduate School of Medicine, Seoul 136-705, Korea

Summary

Polymodal nociceptors detect noxious stimuli including harsh touch, toxic chemicals, and extremes of heat and cold. The molecular mechanisms by which nociceptors are able to sense multiple qualitatively distinct stimuli are not well-understood. We show here that the *C. elegans* PVD neurons are mulitidendritic nociceptors that respond to harsh touch as well as cold temperatures. The harsh touch modality specifically requires the DEG/ENaC proteins MEC-10 and DEGT-1, which represent putative components of a harsh touch mechanotransduction complex. By contrast, responses to cold require the TRPA-1 channel and are MEC-10- and DEGT-1-independent. Heterologous expression of *C. elegans* TRPA-1 can confer cold responsiveness to other *C. elegans* neurons or to mammalian cells, indicating that TRPA-1 is itself a cold sensor. These results show that *C. elegans* nociceptors respond to thermal and mechanical stimuli using distinct sets of molecules, and identify DEG/ENaC channels as potential receptors for mechanical pain.

Introduction

Polymodal nociceptors are sensory neurons that detect aversive stimuli generally perceived as painful. For example, nociceptors respond to harsh touch, extremes of cold and heat, acidic pH, and a variety of toxic chemicals. Although individual nociceptors do not necessarily detect all of these stimuli, the ability to respond to multiple qualitatively distinct aversive cues is a hallmark of both vertebrate and invertebrate nociceptor neurons. Understanding the basis for this polymodality is a fundamental question: are responses to

AUTHOR CONTRIBUTIONS Unless otherwise noted, experiments were conducted and analyzed by M.C. under the guidance of W.R.S. Mammalian TRPA-1 expression and electrophysiology experiments were conducted by S.Y., under the guidance of S.W.H. J.W. generated the microarry data for PVD expression profiling using an mRNA tagging strain constructed by W.C.S.; D.M.M. and M.T. supervised this work and helped with analysis. M.T. first observed the nociceptor-like morphology of PVD. K.S.K. generated the cameleon line for PVD and FLP imaging. W.H.L. initially characterized the harsh touch behavior of *mec-10* and generated the *mec-10; mec-4* double mutants under the guidance of M.D. W.R.S. wrote the paper, with feedback from the other authors.

Europe PMC Funders Author Manuscripts

different stimuli mediated by distinct sets of molecules, or do all responses involve a common polymodal sensory transduction pathway?

Information about the molecular basis of nociceptive sensory transduction has come primarily from studies of two protein superfamilies: the TRP channels and the DEG/ENaC channels [1 2]. TRP channels are non-specific cation channels composed of subunits with six transmembrane α-helices. Several members of the TRP family have been implicated in nociception. For example, TRPV1, the capsaicin receptor, is expressed in mammalian nociceptor neurons and appears to be important for responses to heat, acid, and vanilloid toxins [3 4]. Another TRP channel, TRPM8, is important for sensing cooling as well as cool-mimetic compounds such as menthol [5 6]. Finally, TRPA1, a channel often coexpressed in nociceptors with TRPV1, has been implicated in sensation of noxious cold and a number of chemical irritants as well as non-painful touch, though conflicting results have been obtained for some of these modalities [7 8 9]. At least some TRP channels appear to be sufficient by themselves to produce depolarizing currents in response to thermal, chemical or mechanical stimuli, implicating them as potential primary sensory transducers [10 11 12].

A second family of candidate nociceptive transduction channels are the DEG/ENaC channels. DEG/ENaC channel subunits have two transmembrane α-helices and the heterotrimeric channels they form are permeable to sodium and in some cases calcium [13]. Various members of this family have been linked to sensory transduction processes, including detection of touch, temperature, and acidic pH [14]. The ASIC subfamily in particular has been implicated in the sensation of pain related to tissue acidification [15]. Clear links have also been established between vertebrate and invertebrate DEG/ENaC channels and non-painful mechanosensory processes such as gentle touch [16 17].

Despite significant progress, important questions remain about how painful stimuli are sensed. In particular, the receptor for mechanical pain has not been convincingly identified. Recently, attention has turned to addressing these questions in genetically-tractable invertebrates, such as the nematode *C. elegans*. *C. elegans* contain several neurons with similarities to mammalian polymodal nociceptors. The best characterized are the ASH neurons, ciliated sensory neurons with exposed endings in the animal's nose. The ASH neurons are required for behavioral responses to a variety of aversive stimuli, including noxious chemicals, nose touch, high osmolarity, and acidic pH [18 19]. Calcium imaging experiments indicate that each of these stimuli leads to cell-autonomous activation of neural activity in ASH [20]. Homologues of TRPV (OSM-9) and TRPA (TRPA-1) channels are expressed in ASH, and mutations in the former lead to defects in ASH responses to most aversive stimuli [21 22 23]. *C. elegans* also contain multidendritic neurons (e.g., PVD) that morphologically resemble mammalian nociceptors [24] and express the OSM-9 (TRPV) and TRPA-1 proteins [2123]. In addition, the PVD neurons express the DEG/ENaC protein MEC-10 [25] which contributes to a channel complex that is important for mechanotransduction in body touch neurons [2617]. Cell ablation experiments have implicated the PVD neurons in sensation and avoidance of harsh body touch [27]; roles for the PVD neurons in sensation of other noxious stimuli have not been described.

In this study, we investigated the molecular basis for nociceptive transduction in *C. elegans* multidendritic neurons. We find that the PVD neurons respond to harsh touch as well as cold shock, and are required for avoidance responses to these noxious stimuli. The DEG/ENaC protein MEC-10 is essential for responses to harsh body touch, but is unimportant for responses to cold. A second DEG/ENaC protein, DEGT-1, is also required specifically for harsh touch responses, and may function with MEC-10 in a harsh touch mechanosensory complex. In contrast, responses to acute cold require the TRPA-1 protein, which appears uninvolved in sensing harsh touch. These findings demonstrate that *C. elegans* nociceptors

sense harsh touch and noxious cold using distinct sets of molecules, and identify the MEC-10 DEG/ENaC channel as a candidate receptor for mechanical pain.

Results

PVD multidendritic nociceptors sense harsh touch and cold

The left and right PVD neurons are located on either side of the animal and envelop the body with multidendritic processes similar to those of mammalian nociceptive neurons (Fig. 1a–c). The PVD neurons have been shown to be important for behavioral responses to harsh body touch; in animals lacking the body touch neurons (ALM, AVM, PLM and PVM), PVD ablation significantly compromises escape responses evoked by touching the body with a platinum wire [27]. To test directly whether these neurons respond to harsh touch, we generated a transgenic line expressing the calcium-sensitive fluorescent protein YC2.3 under the control of the *egl-46* promoter. These animals, designated *ljEx19*, expressed the calcium indicator in the PVD neurons as well as another class of multidendritic neurons, the FLPs. Using this line, we observed that calcium transients could be evoked by a harsh mechanical stimulus of large displacement and high velocity (Fig. 1d). In contrast, gentle touch stimuli that activate calcium influx in body touch neurons (e.g. ALM and PLM) did not evoke calcium transients in PVD (Fig. 1e). Thus, the PVD neurons respond specifically to noxious harsh touch.

To determine whether PVD is involved in sensing other noxious stimuli, we ablated the PVD neurons and assayed responses to various conditions that evoke escape behavior. In this way, we found that acute cold shock, administered by changing the buffer temperature from 20° to 15° C, triggered a robust increase in the frequency of omega turns (Fig. 1f), a characteristic avoidance response in which animals change their direction of movement by deep body bending [28 29 30]. PVD-ablated animals were defective in this response to cold, indicating that the PVD neurons are important for cold-shock avoidance (Fig. 1f). We also used the *ljEx19* line to determine whether cold shock induced calcium transients in PVD. We observed that temperature downsteps from 20° to 15° C led to large calcium transients in PVD (Fig. 1g). Calcium changes were not observed in response to smaller temperature downsteps, to 15° to 20° C upsteps, or to temperature upsteps from 20° C to higher temperatures (Supplemental Fig. 1a). Ablations of other neurons, including the AFD thermosensory cells, did not abolish escape responses to 20-15° C cold downsteps (Supplemental Fig. 1b, c). Thus, the PVD neuron specifically responds to acute cold shock as well as to harsh body touch.

MEC-10 is required for harsh touch mechanosensation in PVD

To explore the molecular basis for mechanical and thermal nociception in the PVD neurons, we tested the effects of candidate sensory transduction mutants on calcium transients evoked in response to these stimuli. We first investigated the importance of the DEG/ENaC channel protein MEC-10 in harsh touch mechanosensation. After crossing the *ljEx19* array into a *mec-10(tm1552)* deletion mutant background, we observed that *mec-10(tm1552)* mutants exhibited no detectable calcium transients in response to harsh touch stimulation (Fig. 2a, b). This harsh touch response defect could be rescued by introducing a *mec-10(+)* transgene expressed under the control of the PVD-specific *ser-2prom3* or *egl-46* promoter (Fig. 2c, f, Supplemental Fig. 2a). Harsh touch did not evoke calcium transients in neurons not implicated in harsh touch escape behaviors (Supplemental Fig. 2b). To further evaluate the importance of *mec-10* for harsh touch sensation in PVD, we measured harsh touch avoidance behavior. To focus specifically on the contribution of PVD, we used a *mec-4(u231)* genetic background in which the ALM, AVM and PLM body touch neurons, which respond to gentle as well as harsh touch, were absent [31]. We observed (Supplemental

Fig. 2c) that in this *mec-4(u231)* background, loss of *mec-10* function caused a significant defect in harsh touch avoidance. This harsh touch behavioral defect was rescued by expression of a *mec-10(+)* transgene in the PVD neurons (Supplemental Fig. 2c). Thus, *mec-10* appears to act cell-autonomously in PVD to facilitate a harsh touch response.

We also tested the harsh touch responses of mutants defective in TRP channels expressed in PVD. In contrast to what we had observed for *mec-10* animals, we found that loss-of-function mutants defective in the TRPA channel *trpa-1* or in the TRPV channel *osm-9* showed robust behavioral and PVD calcium responses to harsh touch stimulation (Fig. 2d–f; Supplemental Fig. 2c). Thus, MEC-10 appears to be specifically essential for harsh touch mechanosensation in PVD, while OSM-9 and TRPA-1 are not required for this process.

DEGT-1, a second DEG/ENaC subunit required for harsh touch

What other proteins might contribute to harsh touch mechanosensation in the multidendritic neurons? In contrast to gentle touch, which has been subjected to intense genetic and physiological study, relatively little is known about the molecular basis for harsh touch in *C. elegans*. Since expression of activated MEC-10 without MEC-4 does not produce functional channels in oocytes [3233] MEC-10 may not be able to form homomeric channels. *C. elegans* contains at least 28 DEG channel genes [34], most with uncharacterized expression patterns. Thus, we reasoned that another DEG/ENaC channel protein might function along with MEC-10 in harsh touch mechanoreceptors.

To identify such a protein, we analyzed the results of expression profiling experiments identifying genes with transcripts that are enriched in PVD (Smith, Watson, Spencer, Von Stetina, Treinin, Miller, manuscript in preparation). Among the PVD-enriched genes were four DEG/ENaC channels: *mec-10, del-1, asic-1*, and an uncharacterized gene, F25D1.4 (Supplemental Table 1). *del-1* and *asic-1* deletion alleles had no measurable abnormalities in harsh touch escape behavior or harsh touch-evoked calcium transients in PVD (Supplemental Fig. 3), so we focused our attention on F25D1.4.

Since no deletion allele was available for F25D1.4, we used cell-specific RNAi [35] to eliminate its expression in PVD and assess its effect on harsh touch mechanosensation. We generated multiple transgenic lines (*ljEX224, ljEx225, ljEx258, ljEx264*) that expressed both sense and antisense F25D1.4 sequences (henceforth referred to as RNAi transgenes) cell-specifically in the PVD neurons (Fig. 3, Supplemental Fig. 4a). For the RNAi transgenes, we used two different promoters (*egl-46* and *ser-2prom3*) whose expression domains overlap only in the PVD neurons [3637]. We targeted the F25D1.4 gene using two different segments of the open reading frame, which did not overlap in sequence (Supplemental Fig. 4a, b). Strains carrying any of these PVD-directed F25D1.4 RNAi transgenes completely lacked harsh touch-induced calcium transients as reported by cameleon in PVD (Fig. 3a–d; Supplemental Fig. 4b) and exhibited significant defects in harsh touch escape behavior in a *mec-4(u231)* background (Supplemental Fig. 2c). Both the calcium imaging and behavioral phenotypes of F25D1.4 RNAi animals could be rescued by transgenic expression in PVD of the *C. briggsae* F25D1.4 orthologue (here designated *Cbr-degt-1)*, which shared < 5% sequence identity with the region of *degt-1* targeted by *ljEx225* (Fig. 3c, d). RNAi constructs targeting other PVD-expressed DEG/ENaC channels did not cause a harsh touch defect in PVD, indicating that the harsh touch phenotype resulted from loss of F25D1.4 and not from off-target knockdown of another DEG/ENaC channel (Supplemental Fig. 4c). Expression of F25D1.4 RNAi constructs in other neurons did not cause a harsh touch defect in PVD (Fig. 3d; Supplemental Fig. 4d), nor did the PVD-directed constructs confer harsh touch defects in cells outside the expression domains of their promoters (e.g. ALMs; Supplemental Fig. 4d); thus, the effect of F25D1.4 appeared to be cell-specific. Together, these data indicate that F25D1.4 functions specifically in the PVD

multidendritic neurons in harsh touch mechanosensation. We have designated F25D1.4 *degt-1*, for DEG/ENaC protein involved in touch.

To learn more about the role of DEGT-1 in the PVD neurons, we investigated its intracellular localization by expressing GFP- and RFP-tagged full-length translational fusions (Supplemental Fig. 5a) under the control of the *ser-2prom3* promoter. We observed that both DEGT-1::GFP and DEGT-1::RFP proteins labeled the PVD cell body as well as the PVD dendritic branches in a punctate distribution (Fig. 4a; Supplemental Fig. 6a, b). We also analyzed the localization of a MEC-10::GFP fusion protein (Supplemental Fig. 5b), which rescued the harsh touch defect of the *mec-10(tm1552)* deletion (Supplemental Fig. 5d). We observed a subcellular distribution similar to that of the DEGT-1 fusion proteins, with fluorescence observed in a punctate pattern throughout the dendrite (Fig. 4b, Supplemental Fig. 6c). Colabeling experiments in animals expressing both *degt-1::rfp* and *mec-10::gfp* transgenes in PVD indicated that the DEGT-1 and MEC-10 dendritic puncta colocalize (Fig. 4c–e). These results suggest that the MEC-10 and DEGT-1 proteins are clustered in the PVD dendrites. Significantly, in a *mec-10(tm1552)* mutant background, DEGT-1::RFP became diffusely localized in the PVD dendrite (Fig. 4f–g). This *mec-10*-dependent punctate localization of DEGT-1 parallels the *mec-4*-dependent clustering of MEC-2 in gentle touch neurons [38], and is consistent with the possibility and MEC-10 and DEGT-1 are components of the same harsh touch mechanosensory complex.

MEC-10 and DEGT-1 mediate harsh touch sensation in ALM

In addition to its role in harsh touch, *mec-10* has a well-defined role in gentle touch sensation. Specifically, *mec-10* is important for the responses of body touch neurons such as ALM to low-threshold mechanical stimuli; these responses are also dependent on the DEG/ENaC protein MEC-4 [1725]. ALM neurons respond to harsh touch as well as to gentle touch; while the gentle touch response requires MEC-4, the harsh touch response is MEC-4-independent [39]. This raises the question of whether the role of *mec-10* in harsh touch mechanosensation is a feature of the cell in which it is expressed (PVD instead of ALM) or alternatively a feature of the other molecules with which it associates (DEGT-1 instead of MEC-4).

To address this question, we investigated the effect of *mec-10* on harsh touch responses in the ALM neurons. To determine the importance of MEC-10 for MEC-4-independent harsh touch, we measured the harsh touch-evoked calcium transients in a *mec-4(u253)* null mutant background, in which the ALM neurons are morphologically normal and respond to harsh touch but not gentle touch [39]. We found (Fig. 5a, b, e, Supplemental Fig. 7a) that the ALM calcium responses observed in *mec-4(u253)* single mutants were absent in the *mec-10(tm1552) mec-4(u253)* double mutants. Expression of a wild-type *mec-10(+)* transgene under a touch-neuron-specific promoter restored harsh touch calcium responses (Fig. 5c, e) and partially restored harsh touch avoidance behavior (Supplemental Fig. 7b) to the *mec-10(tm1552) mec-4(u253)* double mutant, indicating that MEC-10 acts cell-autonomously in the ALM neurons. Thus, MEC-10 appears to be essential for harsh touch mechanosensation in ALM as well as PVD.

Based on reporter transgene experiments (Supplemental Fig. 8), *degt-1* is expressed in the ALM neurons; therefore, we also tested the role of DEGT-1 in ALM harsh touch sensation by expressing *degt-1* double-stranded RNA under the control of the *mec-4* promoter. We observed that *degt-1* RNAi largely eliminated harsh touch responses in ALM (Fig. 5d), but did not affect gentle touch responses (Supplemental Fig. 9a, b, d). Thus, while MEC-10 contributes to both the gentle touch and harsh touch modalities of ALM, DEGT-1 appears to be required only for harsh touch. These findings are consistent with the possibility that gentle touch mechanoreceptors contain MEC-4 and MEC-10 subunits, whereas harsh touch

mechanoreceptors contain MEC-10 and DEGT-1. Such a model would predict that overexpression of DEGT-1 might compete with MEC-4 for association with MEC-10, thereby inhibiting gentle touch. In fact, we observed that a multicopy *degt-1* transgene under the control of the *mec-4* promoter significantly compromised gentle touch avoidance and gentle touch-evoked calcium transients in ALM (Supplemental Fig. 9c, d. e). These results are consistent with the possibility that MEC-10 and DEGT-1 function together in a harsh touch mechanosensory complex.

PVD responses to acute cold shock require TRPA-1

We next investigated whether MEC-10 and DEGT-1 are required for PVD responses to other noxious stimuli. In particular, we tested whether loss of either DEG/ENaC channel protein affects responses to cold shock. Calcium imaging experiments in *mec-10* loss-of-function mutant animals revealed no measurable defect in PVD responses to cold downsteps (Supplemental Fig. 10a, g). Likewise, *degt-1* RNAi lines showed normal cold-evoked calcium transients in PVD (Supplemental Fig. 10b, g). Cold-evoked escape behavior was also unaffected by loss of function in either gene (Supplemental Fig. 10d, e). Thus, the DEG/ENaC channel proteins do not affect cold sensation in PVD and appear to be required specifically for responses to noxious touch.

What molecules might be responsible for cold sensation in PVD? Two candidates are TRPA-1 and OSM-9, TRP channels that are expressed in PVD [2321]. To determine the effects of these molecules on cold shock responses, we measured behavioral and calcium imaging responses of *trpa-1(ok999)* and *osm-9(ky10)* animals to temperature downsteps. *osm-9(ky10)* animals responded normally to cold shock (Supplemental Fig. 10c, f, g), indicating that OSM-9 is not required for cold sensation by PVD. However, we observed no cold-evoked calcium transients (Fig. 6a) and no cold-evoked escape behavior (Fig. 6b) in *trpa-1(ok999)* animals. Expression of wild-type *trpa-1(+)* under the control of PVD-specific promoters rescued these cold response defects, indicating that TRPA-1 functions cell-autonomously in the PVD neurons (Fig. 6a, b, d). Since the PVD neurons of *trpa-1* mutants respond normally to harsh touch stimulation (see Fig. 2), the TRPA-1 protein appears to be specifically required for sensation of noxious cold by PVD. These data identify TRPA-1 as a candidate noxious cold thermosensor.

The modality-specific phenotypes of *mec-10, degt-1* and *trpa-1* suggested that mechanosensation and thermosensation occur through functionally distinct pathways in the PVD neurons. To gain further insight into this possibility, we the investigated the intracellular localization of a rescuing (Supplemental Fig. 5c, e) TRPA-1::GFP fusion protein [23] in PVD. We observed that in contrast to MEC-10 and DEGT-1, whose fusion proteins were found in puncta throughout the PVD dendrite, TRPA-1::GFP was restricted to the cell body and the most proximal portion of the dendrite (Fig. 6e, f). This observation suggests that the harsh touch and cold-sensing machinery may not only involve different molecular components but might also be localized differently within the PVD neurons.

Functional conservation between worm and mouse TRPAs

C. elegans TRPA-1 is related to the mammalian mTRPA1 protein, which has been implicated as a potential cold sensor in nociceptor neurons [7]. To assess the functional conservation between *C. elegans* TRPA-1 and its mammalian counterpart, we generated a transgenic line, *ljEx247*, that expressed a mouse mTRPA1 cDNA in the PVD neurons under the control of the *egl-46* promoter. We observed robust calcium transients in response to cold temperature in the PVD neurons of *trpa-1(ok999); ljEx247* animals (Fig. 6c), indicating that mouse mTRPA1 partially rescues the cold-insensitive phenotype of the *trpa-1* deletion mutant. Consistent with the known properties of the mammalian channel, larger responses

were seen following a further temperature downshift to 10° C (Fig. 6c, d). Thus, the mammalian mTRPA1 protein can functionally substitute for *C. elegans* TRPA-1 in nematode neurons.

To further investigate the sufficiency of TRPA-1 for cold sensation, we tested whether heterologous expression of *C. elegans* TRPA-1 could confer cold responsiveness to other cell types. We first expressed *trpa-1* in the *C. elegans* FLP neurons. The FLPs are multidendritic cells with morphological similarities to the PVDs [40]; however, unlike the PVDs, they do not express reporters for *trpa-1* [23] and are activated by heat rather than cold (Fig. 7a, b). When we expressed a *trpa-1* transgene in FLP under the *egl-46* promoter, we observed robust cold-evoked calcium transients (Fig. 7c), indicating that the TRPA-1 protein is sufficient to confer cold responsiveness on the FLP neurons. We also expressed TRPA-1 in the gentle body touch neurons under the control of the *mec-4* promoter. Again, heterologous *trpa-1(+)* expression conferred robust calcium responses to cold shock in the normally cold-insensitive ALM neurons (Fig. 7d–f). These results indicate that TRPA-1 can confer ectopic cold sensing properties on at least two classes of *C. elegans* neurons.

We also tested whether HEK293T cells transiently transefected with *C. elegans* TRPA-1 could be activated by cold stimulation. In whole-cell recordings, we observed robust currents in response to cold stimuli in TRPA-1–expressing HEK cells (n = 9), but not in naive cells (n = 26) (Fig. 8a, c). The average current density evoked by 15°C at + 60 mV was 40.34 ± 19.38 pA/pF (± SEM) in TRPA-1 expressing HEK cells, and 1.78 ± 0.33 pA/pF (± SEM) in untransfected cells (Fig. 8c). Current responses were not observed in response to upstep temperature changes to the room temperature. The currents evoked by cold stimuli in TRPA-1–expressing cells are blocked by gadolinium ions (Supplemental Fig. 11) and show the current-voltage relationship similar to those observed previously at our recording voltages (Fig. 8b and Supplemental Fig. 11) [23]. These results suggest that the TRPA-1 protein is itself sufficient to produce cold-activated cation currents.

Discussion

In this study, we have characterized the sensory transduction pathways of a new class of polymodal nociceptors in the nematode *C. elegans*, the multidendritic PVD neurons. These neurons were previously shown to be important for behavioral responses to harsh touch [27]; the results presented here demonstrate that the PVD neurons are also required for acute behavioral responses to cold, and that both types of noxious stimuli evoke cell autonomous activation of PVD calcium transients. Responses to noxious touch and temperature were shown to require distinct molecular pathways: touch sensation requires the DEG/ENaC proteins MEC-10 and DEGT-1, whereas temperature sensation requires the TRP channel TRPA-1. Thus, polymodal nociception in the *C. elegans* multidendritic neurons appears to involve parallel sensory transduction channels.

The evidence from these studies strongly implicates *C. elegans* TRPA-1 as the thermosensor for cold in the PVD neurons. The effects of the *trpa-1* deletion on the PVD neurons are highly specific to cold responses; moreover, *C. elegans* TRPA-1 protein expressed in mammalian cultured cells is sufficient to produce cold-activated depolarizing currents. These results contrast with previous observations in the OLQ nose touch mechanosensory neurons, in which *trpa-1* was shown to affect touch responses [23]. Why might TRPA-1 affect mechanosensation in one cell type but affect only thermosensation in another? One possibility is that the ability of TRPA-1 channels to function in mechanosensation may depend on the morphology of the cell in which it is expressed. While TRPA-1 channels can be activated by stretch in vitro, the mechanical gating of TRPA channels in vivo may depend on structural features that the PVD neurons lack. Alternatively, TRPA-1 may play an

indirect role in mechanosensation in OLQ, and this function may not be required in other touch-sensing neurons. Interestingly, although heterologous expression of TRPA-1 can confer cold sensitivity on the normally non-responding FLP and ALM neurons, some cells that normally express TRPA1 (e.g. OLQ; Supplemental Fig. 12) do not respond to cold. Thus, the ability of TRPA-1 to mediate neural responses to cold may also depend on additional cell-specific factors.

We have also identified a DEG/ENaC channel that functions specifically in noxious mechanosensation in PVD. We observed that strong mechanical stimuli evoked calcium transients in PVD that were absent in *mec-10* mutants or animals in which a second DEG/ENaC gene, *degt-1*, was knocked down by cell-specific RNAi. MEC-10 and DEGT-1 fusion proteins colocalize in puncta throughout the PVD dendrite, and DEGT-1 localization is *mec-10*-dependent, consistent with the two DEG/ENaC proteins participating in the same multimeric complex. DEGT-1 and MEC-10 may therefore represent essential components of the harsh touch mechanotransducer in PVD. The identity of the receptor for mechanical pain in human polymodal nociceptors is still unknown; based on our results, as well as recent findings from *Drosophila* [41], it is reasonable to speculate that it may be a DEG/ENaC channel.

Our results suggest that subunit composition of DEG/ENaC channels may play an important role in distinguishing harsh touch receptors from gentle touch receptors. Previous work has shown that the ALM body touch neurons contain distinct gentle touch and harsh touch modalities [39], with gentle touch completely dependent on the DEG/ENaC protein MEC-4 and largely dependent on MEC-10 [17]. In contrast, the harsh touch response in ALM requires MEC-10 and DEGT-1, but is independent of MEC-4. Thus, MEC-4/MEC-10 channels may mediate low-threshold responses in the ALM neurons, whereas MEC-4/DEGT-1 channels may mediate high threshold responses within the same cells. Future studies of *mec-4/degt-1* hybrids have the potential to provide insight into the molecular basis for touch sensing by DEG/ENaC complexes.

While these findings are a first step toward identifying the components of the harsh touch mechanotransduction machinery, additional subunits and accessory proteins almost certainly remain to be identified. In particular, stomatin proteins seem to be important components of known DEG/ENaC channel complexes. While MEC-2, the stomatin associated with the gentle touch mechanoreceptor, is not present in the multidendritic neurons, at least two uncharacterized stomatin genes were identified in the PVD expression profile (Smith et al., unpublished). It will be interesting to test the involvement of these proteins in harsh touch-evoked neural activity and behavior. Since harsh touch receptor function can be straightforwardly assessed through both behavioral and neuroimaging assays, it should be possible to identify additional components of the harsh touch mechanoreceptor by assaying candidate gene knockouts or by conducting forward mutant screens.

METHODS

C. elegans Strains

Strains used: AQ2145 *ljEx19[pegl-46::YC2.3 lin-15(+)]*, AQ 2124 *mec-10 (tm1552) mec-4(u231); ljEx19*, AQ2125 *trpa-1(ok999); ljEx19*, AQ 2146 *mec-10(tm1552) mec-4(u253); ljEx19*, AQ2126 *mec-10(tm1552); ljEx19*, AQ2148 *osm-9(ky10); ljEx19*, AQ2143 *del-1(ok1500); ljEx19*, AQ2144 *unc-8(n491n1192); ljEx19*, AQ2284 *trp-4(ok1605); ljEx19*, NC279 *del-1(ok150)*, MT2611 *unc-8(n491n1192)*, AQ906 *bzIs17[pmec-4::YC2.12 lin-15(+)]*, AQ908 *mec-4(u253); bzIs17*, AQ1413 *mec-10(tm1552); bzIs17*, AQ2150 *mec-10(tm1552) mec-4(u2530; bzIs17*, AQ2285 *unc-8(n49n1192); mec-4(u231)*, AQ2286 *del-1(ok150); mec-4(u231) ; ljEx19*, AQ2287 *asic-1(ok415);*

Europe PMC Funders Author Manuscripts

mec-4(u231), AQ2288 *asic-1(ok415); ljEx19*, AQ2270 *mec-10(tm1552); ljEx19; ljEx220[pegl-46::mec-10(+) punc-122::GFP]*, AQ2272 *mec-10(tm1552); ljEx19; ljEx221[pser-2prom3::mec-10(+) punc-122::GFP]*, AQ2273 *mec-10(tm1552); ljEx19; ljEx221*, AQ2280 *ljEx19; ljEx224[pegl-46::degt-1RNAi (Kamath) pmyo-2::GFP]*, AQ2282 *ljEx19; ljEx225[pser-2prom-3::degt-1RNAi (Kamath) pmyo-2::GFP]*, AQ2348 *ljEx246[pegl-46::trpa-1(+)]*, AQ2349 *ljEx247[pegl-46::mTRPA1]*, NC1687 *wdIs52[PF49H12.4::GFP unc-119(+)]* AQ2396 *ljEx250[pser-2prom3::mec-10::GFP; pmyo-2::GFP]*, AQ2400 *ljEx254[pser-2prom3::degt-1::GFP pmyo-2::GFP]*, AQ2402 *ljEx256[pser-2prom3::degt-1::mCherry pmyo-2::GFP]*, *AQ2404 ljEx258[pser-2prom3::degt-1RNAi (Sonnichsen) pmyo-2::GFP]; ljEx19*, AQ2405 *ljEx259[pser-2prom3::asic-1RNAi; pmyo-2::GFP]; ljEx19*, AQ2406 *ljEx260[pser-2prom3::unc-8RNAi pmyo-2::GFP]; ljEx19*, AQ2407 *ljEx225; ljEx19; ljEx261[pser-2prom3::Cbr-degt-1 punc-122::GFP]*, AQ2408 *ljEx19; ljEx262[pegl-46::mTRPA-1 pmyo-2::GFP]*, AQ2409 *bzIs17*, *ljEx263[pmec-4::trpa-1(+); pmyo-2::GFP]*, AQ2410 *ljEx19; ljEx264[pegl-46::degt-1RNAi (Sonnichsen) pmyo-2::GFP]*, AQ2411 *ljEx258; ljEx19; ljEx261*, AQ2412 *ljEx234; ljEx19; ljEx261*, AQ2413 *ljEx266[pmec-4::Cbr-degt-1 punc-122::GFP]*, AQ2414 *bzIs17; ljEx265[pmec-4::degt-1RNAi(Sonnichsen) pmyo-2::GFP]*, AQ2415 *bzIs17; ljEx265; ljEx266*, AQ2416 *bzIs17; ljEx240[pmec-4::degt-1 RNAi (Kamath) pmyo-2::GFP]; ljEx266* AQ2417 *mec-10(tm1552); ljEx19; ljEx230[pser-2prom-3::mec-10(cDNA)]*, AQ1044 *ljEx95 [psra-6::yc2.12; lin-15(+)]*, AX1907 *[pgcy32::YC3.60]*, AQ2427 *ljEx250; ljEx256*, AQ2428 *ljEx267[pser-2prom3::trpa-1::GFP pmyo-2::GFP];* AQ2437 *bzIs17; ljEx240;* AQ2435 *bzIs17; ljEx268[pmec-4::degt-1(+) pmyo-2::GFP]*, AQ2436 *mec-10(tm1552) mec-4(u2530); bzIs17; ljEx228[pmec-4::mec-10(+) pmyo-2::GFP]*

Generation of FLP/PVD cameleon line *ljEx19*

The *egl-46* promoter region was obtained from plasmid TU#307 [37], a gift from the lab of Martin Chalfie. A 3 kb HinDIII/NotI fragment was fused to cameleon YC2.3 in the vector pPD95.75 (A. Fire). Transgenic lines were obtained by germline injection of a *lin-15(n765)* mutant strain with the *egl-46::YC2.3* plasmid at a concentration of 50 ng/μl along with *lin-15(+)* genomic DNA (30 ng/μl) as a coinjection marker. Once a stable transgenic line was obtained, the *lin-15(n765)* allele was removed by backcrossing to wild-type (N2) animals.

Transgenic rescue lines

For all rescue plasmids, we used the MultiSite Gateway Three Fragment Vector Construction Kit. Individual PCR products were cloned into the appropriate pDONOR vector generating pENTRY clones. Subsequently, pENTRY vectors with the promoter and gene of interest as well as an *unc-54* 3′UTR containing vector were recombined with a pDEST vector in order to generate an Expression vector.

For rescue arrays *ljEx219, ljEx220*, and *ljEx221*, a 4.4kb *mec-10* genomic DNA was amplified using Phusion High- Fidelity DNA Polymerase F-530S from adult genomic DNA using the primers 5′-GTACAAAATTCAAAAAATGAATCG-3′ and 5′-GAAATAAGAAATTTATTTTCCG-3′. For *ljEx261* and *ljEx266*, a 4.4kb region coding for *C. briggsae degt-1* orthologue *Cbr-degt-1* was amplified from adult genomic DNA with the primers 5′- ATGCCCCGAAAACGAAGGTCTG-3′ and 5′-CACATCATATTGATGGGTTGGTG-3′. For array *ljEx230*, a 2.2kb *mec-10* cDNA was amplified using Qiagen OneStep RT-PCR Kit from an RNA library using the primers 5′-ATGAATCGAAACCCGCGAATG-3′ and 5′-TCAATACTCATTTGCAGCATTTTC-3′. For array *ljEx246*, a *trpa-1* 3.6kb cDNA fragment was amplified from a plasmid generated previously [23] using the primers 5′-ATGTCGAAGAAATCATTAGG-3′ and 5′-

TCAGTTATCTTTCTCCTCAAGT-3′. A 1kb *mec-4* promoter region was obtained from plasmid pIR13, a gift from I. Rabinowitch from the Schafer lab. The 1.7 kb *ser-2prom-3* was obtained from plasmid pWCS8, from the Miller lab. We used the same *egl-46* promoter fragment described above in the creation of the *egl-46*::cameleon plasmid.

The *pmec-4::mec10* construct was injected in *mec-10(tm1552); ljEx19 [pegl-46::YC2.3]* animals at 72 ng/μl with *punc122::GFP* at 20 ng/μl to generate array *ljEx219[pmec-4::mec-10 punc122::GFP]*. The same *pmec-4::mec10* construct was injected in *mec-10(tm1552); bzIs17* animals at 70 ng/μl with *pmyo-2::GFP* at 20 ng/μl to generate array *ljEx228[pmec-4::mec-10 pmyo-2::GFP]*. This was crossed into the *mec-10(tm1552) mec-4(u253)* double mutant to generate strain AQ2436. We injected *mec-10(tm1552); ljEx19[pegl-46::YC2.3]* worms with *pegl-46::mec-10* at 80 ng/μl and with *punc122::GFP* at 20 ng/μl to generate array *ljEx220 [pegl-46::mec-10 punc122::GFP]*. To generate cell-specific rescue of *mec-10* in the PVD cells, we injected *mec-10(tm1552); ljEx19[pegl-46::YC2.3]* worms with *ser-2prom-3::mec-10* at 80 ng/μl with *punc122::GFP* at 20 ng/μl to generate array *ljEx221* transgenic worms. A *pegl-46::trpa-1* construct which injected into wild-type at 70 ng/μl with *punc122::GFP* at 20 ng/μl to generate array *ljEx246*. A *pser-2prom3frag-2::trpa-1* construct was injected into wild-type *ljEx19[pegl-46::YC2.3]* animals at 70 ng/μl with *pmyo-2::GFP* at 11ng/μl to generate array *ljEx245*. These animals were crossed into the *degt-1RNAi* strains AQ2282 and AQ2404.

Cell Ablations

Laser ablations were carried out using a standard protocol [42]. The FLPs and AFDs, PLMs, and ASHs were ablated in the early L1 stage, usually 3-4 hr post hatching; the PVD cells were ablated at early L2. As an additional control, we also ablated V5 precursor cells at early L1 stage which removes the PVD/PDE cells (data not shown); no significant difference in the effects of the two different ablations was noted. All ablations were confirmed by observing loss of cameleon fluorescence in the adult animal.

Generation of *degt-1* and control RNAi lines:

Transgenes for cell-specific knockdown were constructed as described [35]. *ljEx224[pegl-46::degt-1RNAi]* and *ljEx225[ser-2prom-3::degt-1RNAi]* expressed a *degt-1(RNAi)* in the FLP and PVD, or OLL and PVD neurons respectively. Transgene *ljEx240[pmec-4::degt-1 RNAi]* expressed a *degt-1 RNAi* transgene in the gentle body touch neurons (ALM, AVM, PLM, PVM). For these constructs, the same exon-rich region of *degt-1* that was used as an insert for the Kamath et al. RNAi feeding library [43] was amplified using the primers 5′-CGGTTGTAAACATGACGCTG-3′ and 5′-CCACGGATGAATCGAGTTTT-3′. A second set of RNAi lines against *degt-1* targeting a different region of the gene was generated by using the exon rich region of *degt-1* that was used as an insert for the Sonnichsen et al. RNAi feeding library [44]. The following primers: 5′- CTAACCCACCATTTCCGCTA-3′ and 5′-TTGCGTGGTTATTCTTTCCC-3′ amplified a 1.7 kb fragment from which three different transgenes were generated: *ljEx265[pmec-4::degt-1 RNAi]*, *ljEx258[pegl-46::degt-1RNAi]* and *ljEx225[ser-2prom-3::degt-1RNAi]* expressed a *degt-1(RNAi)* in the body touch neurons, FLP and PVD, or OLL and PVD neurons respectively. For all RNAi transgenes, both sense and antisense expression clones were microinjected at 100 ng/μl together with 50 ng/μl *pmyo-2::GFP* as a coinjection marker.

PVD expression profiling

A 1.6 kb region of the *ser-2prom3* promoter [36] was inserted into the 3XFLAG::PAB-1 plasmid, pSV15 [45] to produce the *ser-2prom3B*::3XFLAG::PAB-1 mRNA tagging construct pWCS8. A transgenic line (*NC221*) was generated by microparticle bombardment and

specific expression in PVD and OLL neurons confirmed by antiFLAG immunostaining. The mRNA tagging method was used to isolate PVD/OLL transcripts from synchronized L3-L4 larvae [46]. A reference sample of total RNA from all larval cells was obtained from L3-L4 larval lysates by trizol extraction. Triplicate samples were applied to the Affymetrix Gene Chip array and transcripts showing relative enrichment (> 1.5X; false discovery rate (FDR) < 1%) in PVD/OLL vs the reference were identified using previously described methods [4748]. Four DEG/ENaC channel transcripts (*mec-10, del-1, asic-1, degt-1*) satisfied these criteria whereas *mec-4* showed only slight enrichment (1.1 X) at relaxed stringency (< 10% FDR) (Table 1). A detailed description of these methods and a comprehensive analysis of the microarray results will be presented elsewhere (Smith et al., manuscript in preparation).

Generation of DEGT-1, MEC-10 and TRPA1 fusion protein transgenes

Fusion transgenes were expressed under the control of the *ser-2prom3* promoter described above. Primers to PCR-amplify the genomic regions coding for MEC-10, DEGT-1 and TRPA-1 were altered to allow in frame fusion with the C-terminal tag. pENTRY clones for GFP and mCherry-RFP were generated in the lab by Ithai Rabinowitch (unpublished). Transgenic lines were generated by injecting the constructs into the N2 strain; each line was compared with multiple additional independently-derived transgenic lines with the same transgene in order to confirm the reproducibility of the expression pattern. The *mec-10::GFP* construct was injected at 95 ng/μl with *pmyo-2::GFP* at 11 ng/μl, giving *ljEx250*. The *degt-1::GFP* construct was injected at 86 ng/μl with pmyo-2::GFP at 15 ng/μl, giving *ljEx254*. The *degt-1::mCherry* construct was injected at 100 ng/μl with *pmyo-2::GFP* at 15 ng/μl, giving *ljEx256*. The *trpa-1::GFP* construct was injected at 60 ng/μl with pmyo-2::GFP at 15 ng/μl, giving *ljEx267*. In order to test for functional rescue, the transgenic lines were crossed into the corresponding mutant background and subsequently tested for touch or cold responses.

Calcium Imaging

Optical recordings were performed essentially as described [4950] on a Zeiss Axioskop 2 upright compound microscope equipped with a Dual View beam splitter and a Uniblitz Shutter. Fluorescence images were acquired using MetaVue 6.2. Filter-dichroic pairs were excitation, 400–440; excitation dichroic 455; CFP emission, 465–495; emission dichroic 505; YFP emission, 520–550. Individual adult worms (~24h past L4) were glued with Nexaband S/C cyanoacrylate glue to pads composed of 2% agarose in extracellular saline (145 mM NaCl, 5 mM KCl, 1 mM CaCl2, 5 mM MgCl2,20 mM D-glucose, 10 mM HEPES buffer, pH 7.2). Worms used for calcium imaging had similar levels of cameleon expression in sensory neurons as inferred from initial fluorescence intensity. Acquisitions were taken at 28Hz (35ms exposure time) with 4×4 or 2×2 binning, using a 63x Zeiss Achroplan water immersion objective.

Gentle body touch stimulation was performed as described [39], with a standard probe displacement of ~10 μm. Harsh stimuli were delivered using a glass needle with a sharp end (the outcome of these experiments was the same if a piece of platinum wire was used). which was driven into the worm ~30 to 50 μm at speed of 2.8 μm/s. Stimulus duration was ~50 ms.

For thermal stimulation, a circular metal stage (Microscope Thermal Stage MTS-1, Techne, Proton-Wilten, Antwerpen, Belgium) was fitted with four 80 W peltier elements controlled by a National Instruments controller and custom-made Labview software. A T-junction thermocoupler located inside the chamber where the worm is positioned provides a continuous stream of readings to the temperature controller and adjusts the temperature using a feedback system. A worm grown at 20° C was glued on an agar pad (2%) in a

buffer-filled chamber with an approximate volume of 0.5 ml. The aquisition rate was 28Hz; the recordings lasted 2 minutes with a 30 second stimulus.

Behavioral Assays

For harsh body touch, animals were touched at the midsection of the body with a platinum wire. Animals were stimulated and were scored for reversal behavior, with a 3 minute interval between each stimulus. 100 animals were assayed from each genotype. Thermal avoidance was assayed essentially as described[30]. We used the same thermal controller system described for the calcium imaging experiments. To improve the contrast we provided dark-field illumination using a paired fiber-optic gooseneck lamp set at an oblique angle. The worm swims freely in a microdroplet sandwiched between a cover slip from below and a round sapphire window from above. A typical microdroplet contained ~0.6 μL of neuronal buffer that flattens to a circular droplet containing a young adult worm. Using a 20X air objective we recorded for 350 seconds at 10 frames per second. Worms cultivated at 20°C were recorded initially for 150 seconds at 20°C; the stimulus (a fast drop in temperature to 15°C) lasted 60 seconds followed by a return to 20°C. Image stacks were loaded on ImageJ and were scored blindly for omega turns according to the criteria described previously [30]. Events following a previous event within 0.3 seconds were rejected.

TRPA-1 expression in mammalian cells

HEK293T cells were maintained in DMEM containing 10% FBS and 1% penicillin/ streptomycin. The HEK cells were transiently transfected with 3 μg of TRPA-1 channel plasmid DNA per 35 mm dish using Fugene 6 (Roche Diagnostics, Indianapolis, IN) as described [23]. Cells were plated onto poly-D-lysine–coated coverslips for recording purposes, and we made recordings 10-24 h after transfection.

Whole-cell voltage clamp recordings were performed with protocols slightly modified from those described previously[23]. Briefly, the bath solution contained 140 mM NaCl, 5 mM KCl, 2 mM CaCl2, 1 mM MgCl2, 10 mM HEPES, titrated to pH 7.4 with NaOH. The pipette solution contained 140 mM CsCl, 5 mM EGTA, 10 mM HEPES, 2.0 mM MgATP, 0.2 mM NaGTP titrated to pH 7.2 with CsOH. The holding potential was −60 mV and for the current-voltage analysis, 800ms voltage-ramp pulses from −80 to +80 mV were used. For cold temperature stimulation, Bipolar Temperature Controller CL-100 (Warner Instruments, Hamden, CT) was used. The temperature was measured using a temperature probe (TA-29, Warner Instruments) located ~5 mm distant from the cells under recording.

Confocal microscopy

PVDL labeled with F49H12.4::GFP [48] was imaged in a Zeiss LSM 510 Meta confocal microscope with a 40X objective. The MEC-10::GFP, DEGT-1::GFP, DEGT-1::mCherry and TRPA-1::GFP lines were imaged in a Zeiss LSM 510 Meta confocal microscope with a 60X objective.

Supplementary Material

Refer to Web version on PubMed Central for supplementary material.

Acknowledgments

We thank the Caenorhabditis Genetics Center, the National Bioresource Project and the Mitani lab for strains, N. Barry for help with microscopy, I. Rabinowitz for writing software to analyze averaged ratio traces, D. Cattermole and P. Heard in the LMB technical workshop for designing and building thermal controllers, the Vanderbilt Functional Genomics Shared Resource for help with microarray experiments, and R. Branicky for comments on the manuscript. This research was supported by the Medical Research Council and grants from NIDA (W.R.S) and

NINDS (M.D. and D.M.M), from the Brain Research Center of the 21st Century Frontier Research Program funded by the Ministry of Education, Science and Technology of Korea [code M103KV010015-06K2201-01510] and National Research Foundation of Korea [code KRF-2008-331-E00457 and 2009-0076543] to S.W.H, and from the US-Israel Binational Science Foundation (Grant 2005036 to M.T. and D.M.M.).

REFERENCES

1. Patapoutian A, Tate S, Woolf CJ. Transient receptor potential channels: targeting pain at the source. Nat Rev Drug Discov. 2009; 8:55–68. [PubMed: 19116627]
2. Wemmie JA, Price MP, Welsh MJ. Acid-sensing ion channels: advances, questions and therapeutic opportunities. Trends Neurosci. 2006; 29:578–86. [PubMed: 16891000]
3. Caterina MJ, et al. The capsaicin receptor: a heat-activated ion channel in the pain pathway. Nature. 1997; 389:816–24. [PubMed: 9349813]
4. Tominaga M, et al. The cloned capsaicin receptor integrates multiple pain-producing stimuli. Neuron. 1998; 21:531–43. [PubMed: 9768840]
5. McKemy DD, Neuhausser WM, Julius D. Identification of a cold receptor reveals a general role for TRP channels in thermosensation. Nature. 2002; 416:52–8. [PubMed: 11882888]
6. Peier AM, et al. A TRP channel that senses cold stimuli and menthol. Cell. 2002; 108:705–15. [PubMed: 11893340]
7. Story GM, et al. ANKTM1, a TRP-like channel expressed in nociceptive neurons, is activated by cold temperatures. Cell. 2003; 112:819–29. [PubMed: 12654248]
8. Bandell M, et al. Noxious cold ion channel TRPA1 is activated by pungent compounds and bradykinin. Neuron. 2004; 41:849–57. [PubMed: 15046718]
9. Bautista DM, et al. TRPA1 mediates the inflammatory actions of environmental irritants and proalgesic agents. Cell. 2006; 124:1269–82. [PubMed: 16564016]
10. Christensen AP, Corey DP. TRP channels in mechanosensation: direct or indirect activation? Nat Rev Neurosci. 2007; 8:510–21. [PubMed: 17585304]
11. Kahn-Kirby AH, Bargmann CI. TRP channels in C. elegans. Annu Rev Physiol. 2006; 68:719–36. [PubMed: 16460289]
12. Kang K, et al. Analysis of Drosophila TRPA1 reveals an ancient origin for human chemical nociception. Nature. 464:597–600. [PubMed: 20237474]
13. Bounoutas A, Chalfie M. Touch sensitivity in Caenorhabditis elegans. Pflugers Arch. 2007; 454:691–702. [PubMed: 17285303]
14. Garcia-Anoveros J, Corey DP. The molecules of mechanosensation. Annu Rev Neurosci. 1997; 20:567–94. [PubMed: 9056725]
15. Price MP, et al. The DRASIC cation channel contributes to the detection of cutaneous touch and acid stimuli in Mice. Neuron. 2001; 32:1071–1083. [PubMed: 11754838]
16. Driscoll M, Chalfie M. The *mec-4* gene is a member of a family of *Caenorhabditis elegans* genes that can mutate to induce neuronal degeneration. Nature. 1991; 349:588–593. [PubMed: 1672038]
17. O'Hagan R, Chalfie M, Goodman MB. The MEC-4 DEG/ENaC channel of Caenorhabditis elegans touch receptor neurons transduces mechanical signals. Nat Neurosci. 2005; 8:43–50. [PubMed: 15580270]
18. Kaplan JM, Horvitz HR. A dual mechanosensory and chemosensory neuron in Caenorhabditis elegans. Proc Natl Acad Sci U S A. 1993; 90:2227–31. [PubMed: 8460126]
19. Hilliard MA, Bergamasco C, Arbucci S, Plasterk RH, Bazzicalupo P. Worms taste bitter: ASH neurons, QUI-1, GPA-3 and ODR-3 mediate quinine avoidance in Caenorhabditis elegans. Embo J. 2004; 23:1101–11. [PubMed: 14988722]
20. Hilliard MA, et al. In vivo imaging of C. elegans ASH neurons: cellular response and adaptation to chemical repellents. Embo J. 2005; 24:63–72. [PubMed: 15577941]
21. Colbert HA, Smith TL, Bargmann CI. OSM-9, a novel protein with structural similarity to channels, is required for olfaction, mechanosensation, and olfactory adaptation in *C. elegans*. J. Neurosci. 1997; 17:8259–8269. [PubMed: 9334401]

Europe PMC Funders Author Manuscripts

22. Tobin D, et al. Combinatorial expression of TRPV channel proteins defines their sensory functions and subcellular localization in C. elegans neurons. Neuron. 2002; 35:307–18. [PubMed: 12160748]
23. Kindt KS, et al. Caenorhabditis elegans TRPA-1 functions in mechanosensation. Nat Neurosci. 2007; 10:568–77. [PubMed: 17450139]
24. Yassin L, Samson AO, Halevi S, Eshel M, Treinin M. Mutations in the extracellular domain and in the membrane-spanning domains interfere with nicotinic acetylcholine receptor maturation. Biochemistry. 2002; 41:12329–35. [PubMed: 12369821]
25. Huang M, Chalfie M. Gene interactions affecting mechanosensory transduction in *Caenorhabditis elegans*. Nature. 1994; 367:467–470. [PubMed: 7509039]
26. Chelur DS, et al. The mechanosensory protein MEC-6 is a subunit of the C. elegans touch-cell degenerin channel. Nature. 2002; 420:669–73. [PubMed: 12478294]
27. Way JC, Chalfie M. The mec-3 gene of Caenorhabditis elegans requires its own product for maintained expression and is expressed in three neuronal cell types. Genes Dev. 1989; 3:1823–33. [PubMed: 2576011]
28. Croll NA. Components and patterns in the behaviour of the nematode, Caenorhabditis elegans. J Zool, Lond. 1975; 176:159–176.
29. Gray JM, Hill JJ, Bargmann CI. A circuit for navigation in Caenorhabditis elegans. Proc Natl Acad Sci U S A. 2005; 102:3184–91. [PubMed: 15689400]
30. Srivastava N, Clark DA, Samuel AD. Temporal analysis of stochastic turning behavior of swimming C. elegans. J Neurophysiol. 2009; 102:1172–9. [PubMed: 19535479]
31. Driscoll M, Chalfie M. The mec-4 gene is a member of a family of Caenorhabditis elegans genes that can mutate to induce neuronal degeneration. Nature. 1991; 349:588–93. [PubMed: 1672038]
32. Goodman MB, et al. MEC-2 regulates C. elegans DEG/ENaC channels needed for mechanosensation. Nature. 2002; 415:1039–42. [PubMed: 11875573]
33. Bianchi L, et al. The neurotoxic MEC-4(d) DEG/ENaC sodium channel conducts calcium: implications for necrosis initiation. Nat Neurosci. 2004; 7:1337–44. [PubMed: 15543143]
34. Goodman, MB. WormBook. Community, T. C. e. R.. , editor. 2006.
35. Esposito G, Di Schiavi E, Bergamasco C, Bazzicalupo P. Efficient and cell specific knock-down of gene function in targeted C. elegans neurons. Gene. 2007; 395:170–6. [PubMed: 17459615]
36. Tsalik EL, et al. LIM homeobox gene-dependent expression of biogenic amine receptors in restricted regions of the C. elegans nervous system. Dev Biol. 2003; 263:81–102. [PubMed: 14568548]
37. Wu J, Duggan A, Chalfie M. Inhibition of touch cell fate by egl-44 and egl-46 in C. elegans. Genes Dev. 2001; 15:789–802. [PubMed: 11274062]
38. Zhang S, et al. MEC-2 is recruited to the putative mechanosensory complex in C. elegans touch receptor neurons through its stomatin-like domain. Curr Biol. 2004; 14:1888–96. [PubMed: 15530389]
39. Suzuki H, et al. In vivo imaging of C. elegans mechanosensory neurons demonstrates a specific role for the MEC-4 channel in the process of gentle touch sensation. Neuron. 2003; 39:1005–17. [PubMed: 12971899]
40. Hall, D.; Altun, ZF. *C. elegans* atlas. Cold Spring Harbor Laboratory Press; Cold Spring Harbor, NY: 2008.
41. Zhong L, Hwang RY, Tracey WD. Pickpocket is a DEG/ENaC protein required for mechanical nociception in Drosophila larvae. Curr Biol. 20:429–34. [PubMed: 20171104]
42. Bargmann CI, Avery L. Laser killing of cells in *Caenorhabditis elegans*. Meth. Cell Biol. 1995; 48:225–250.
43. Kamath RS, Martinez-Campos M, Zipperlen P, Fraser AG, Ahringer J. Effectiveness of specific RNA-mediated interference through ingested double-stranded RNA in Caenorhabditis elegans. Genome Biol. 2001; 2 RESEARCH0002.
44. Sonnichsen B, et al. Full-genome RNAi profiling of early embryogenesis in Caenorhabditis elegans. Nature. 2005; 434:462–9. [PubMed: 15791247]

45. Von Stetina SE, et al. UNC-4 represses CEH-12/HB9 to specify synaptic inputs to VA motor neurons in C. elegans. Genes Dev. 2007; 21:332–46. [PubMed: 17289921]
46. Von Stetina SE, et al. Cell-specific microarray profiling experiments reveal a comprehensive picture of gene expression in the C. elegans nervous system. Genome Biol. 2007; 8:R135. [PubMed: 17612406]
47. Fox RM, et al. A gene expression fingerprint of C. elegans embryonic motor neurons. BMC Genomics. 2005; 6:42. [PubMed: 15780142]
48. Watson JD, et al. Complementary RNA amplification methods enhance microarray identification of transcripts expressed in the C. elegans nervous system. BMC Genomics. 2008; 9:84. [PubMed: 18284693]
49. Kerr R, et al. Optical imaging of calcium transients in neurons and pharyngeal muscle of C. elegans. Neuron. 2000; 26:583–94. [PubMed: 10896155]
50. Kerr RA. Imaging the activity of neurons and muscles. WormBook. 2006:1–13. [PubMed: 18050440]

Europe PMC Funders Author Manuscripts

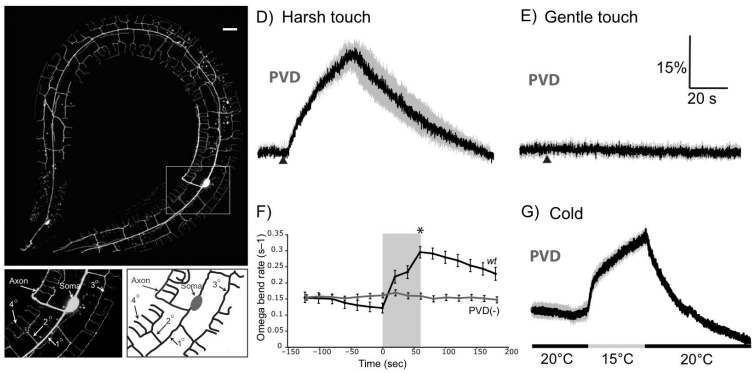

Figure 1. PVD neurons respond to harsh touch and cold temperature.

a–c. PVD neurons display complex dendritic arbors that envelop the animal. Confocal Z-projection of adult (left side) showing PVDL labeled with F49H12.4::GFP marker (anterior to left, ventral side corresponds to inside surface of looped worm). PVDR on the right side is excluded from this confocal series. Insets show enlarged view of posterior-lateral location of PVDL cell soma with ventrally projecting axon and orthogonal array of dendritic branches. Scale bar in panel A is 15 μm. **d–e. Calcium responses to harsh (d) and gentle (e) touch.** Each red trace represents the average percentage change in normalized YFP/CFP ratio (R/R_0) for 20 individual recordings. The black triangle indicates the time at which the mechanical stimulus (see Methods) was applied. Gray shading indicates SEM of the mean response. **f. Behavioral responses to cold shock**. Shown are percentages of animals (n=30) displaying avoidance behavior (omega bends) during a recording of animals experiencing acute temperature change (20-15° C). The blue box indicates a 50 second interval during which the buffer temperature was 15° C; temperature was 20° C during the remainder of the recording. Error bars indicate SEM; PVD- animals (in which both PVD neurons ablated by laser microsurgery) were significantly less responsive than intact animals (* $P < .05$) according to the Student's t test. **g. Calcium response to cold shock**. Red trace represents the average percentage change in R/R_0 for 20 individual recordings; gray shading indicates SEM of the mean response. The lower line indicates the buffer temperature during the recording.

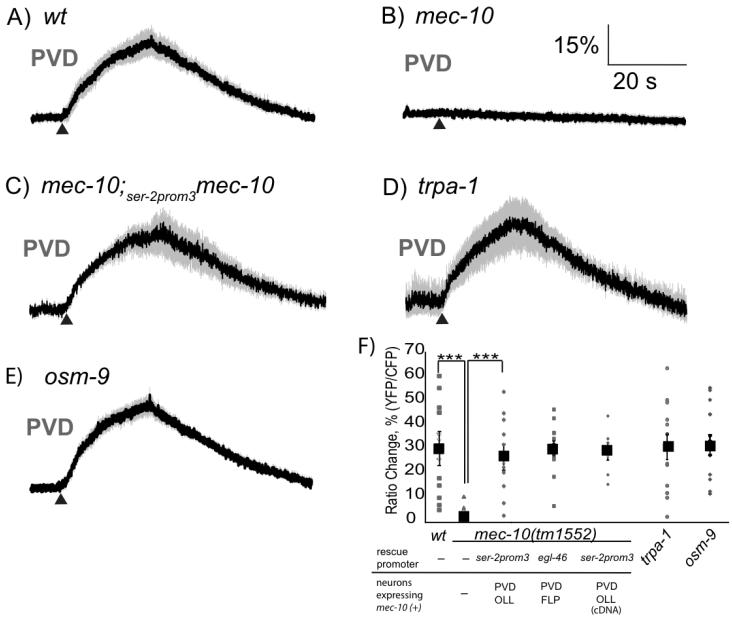

Figure 2. *mec-10* is required for harsh touch in PVD

a–b *mec-10(tm1552)* animals are defective in harsh touch response in PVD. Shown are averaged responses of 17 wild-type (a), and 14 *mec-10(tm1552)* mutant (b) animals to harsh body touch. For these and other panels, the red trace represents the average percentage change in normalized YFP/CFP ratio (R/R_0); gray shading indicates SEM of the mean response. Scale bars are indicated in upper left. The triangle indicates the time of the stimulus. **c. PVD-specific rescue of the *mec-10* harsh touch phenotype.** Shown is the averaged calcium response of 13 *mec-10(tm1552); ljEx*221 *[pser-2prom-3::mec-10(+)]* animals. Rescue was also observed with a *mec-10* cDNA and with a second PVD-specific promoter, *pegl-46* (see panel F). **d–e. *trpa-1* and *osm-9* are not required for harsh touch in PVD.** Shown are averaged traces for 13 *trpa-1(ok999)* (D) and 17 *osm-9(ky10)* (E) animals. **f. Scatter plot of peak calcium responses for each genotype.** Statistical significance (*** $p < .0005$) is according to the Mann-Whitney rank sum test. Additional genotypes shown include *mec-10(tm1552); ljEx220 [pegl-46::mec-10(+)]* (13 recordings) and mec-10(tm1552); ljEx230 [pser-2prom-3::mec-10(cDNA)] (12 recordings).

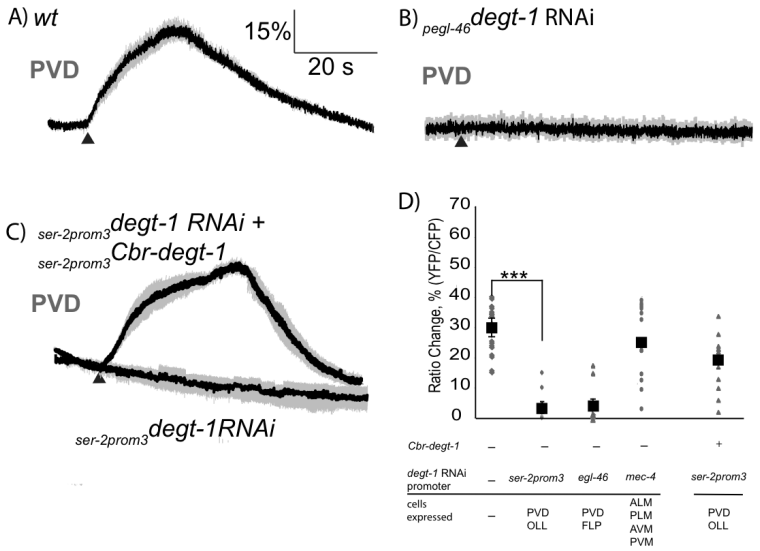

Figure 3. DEGT-1 is required for harsh touch responses in PVD

a–c. Calcium responses of wild-type and *degt-1RNAi* animals to harsh body touch in PVD. Each red trace represents the average percentage change in normalized YFP/CFP ratio (R/R_0) for the indicated genotype; gray shading indicates SEM of the mean response. Panel a shows wild-type response (13 animals recorded). Panels b and c show loss of harsh touch response in lines expressing *degt-1* RNAi under the PVD-specific promoters *pegl-46* (*ljEx224*; 14 animals) and *pser-2prom3* (*ljEx225*; 17 animals). In panel c, the green line shows rescue of the *pser-2::degt-1RNAi* (*ljEx225*) phenotype by the *C. briggsae* orthologue *Cbr-degt-1* expressed cell-specifically in PVD under the control of the *pser-2prom3* promoter (*ljEx261*; 14 animals). *Cbr-degt-1* shares less than 5% sequence identity with *C. elegans degt-1* over the region targeted by *ljEx225*. **d. Scatter plot of peak calcium responses for each genotype.** Statistical significance (*** $p < .001$) is according to the Mann-Whitney rank sum test. Also shown are responses of the off-target control in which a *degt-1* RNAi transgene is expressed outside PVD under the touch neuron promoter *pmec-4* (*ljEx240*; 14 animals recorded). Responses of additional on-target and off-target RNAi control strains are shown in Supplemental Figure 4.

Europe PMC Funders Author Manuscripts

Europe PMC Funders Author Manuscripts

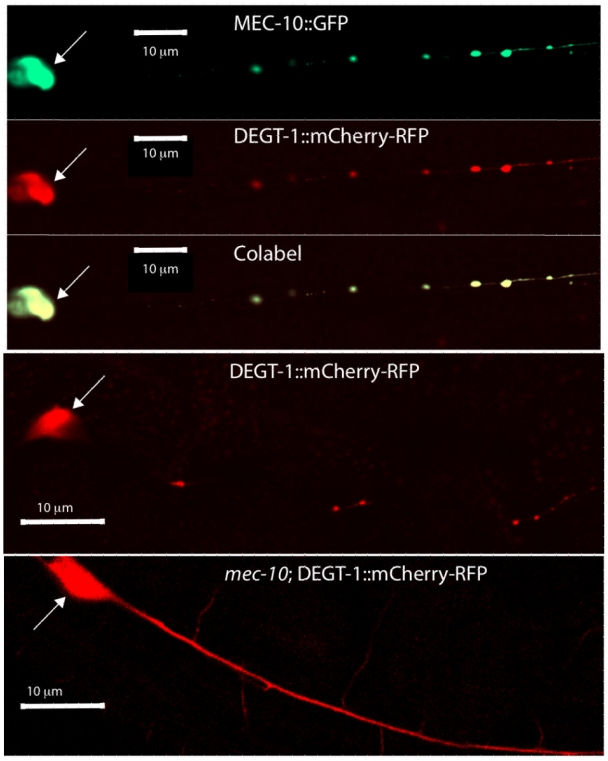

Figure 4. Localization patterns of DEGT-1 and MEC-10 fusion proteins in PVD

For all figures, the large arrows indicate the PVD soma. **a–c. Colocalization of MEC-10::GFP and DEGT-1::RFP in PVD dendritic puncta.** Shown are green, red, and dual wavelength images of a single confocal section of AQ2427 *ljEx250[pser-2prom3::mec-10::GFP; pmyo-2::GFP]; ljEx256[pser-2prom3::degt-1::mCherry pmyo-2::GFP]* animals, which express both MEC-10::GFP and DEGT-1::RFP in PVD. AQ2427 was generated by crossing AQ2396 *ljEx250* and AQ2402 *lj256*, and selecting for the presence of both arrays. These images all show the primary PVD dendrite; similar results were observed in higher-order dendritic branches (Supplemental Figure 6). **d–e. Punctate localization of DEGT-1::RFP is *mec-10*-dependent.** Shown are single confocal sections of PVD processes expressing the *ljEx256* DEGT-1::RFP transgene in a wild-type (d) or *mec-10(tm1552)* mutant (e) background. *degt-1* RNAi did not abolish punctate expression of MEC-4::GFP (Supplemental Figure 6).

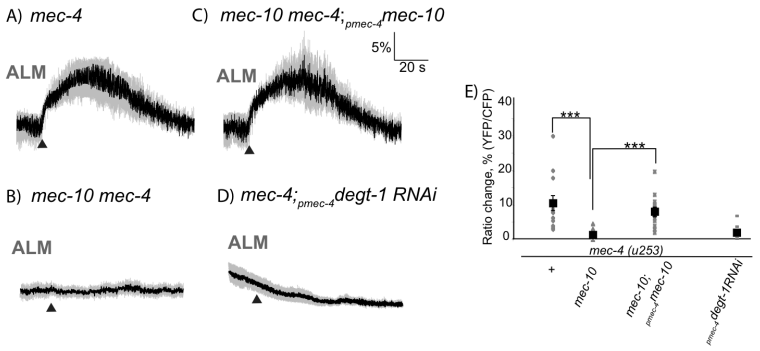

Figure 5. Effect of *mec-10* on harsh touch responses in ALM

a–b. *mec-10* is required for *mec-4*-independent harsh touch response in ALM. Shown are calcium responses in ALM to fast large-displacement stimulation in *mec-4(u253)* single mutant (a) and *mec-10(tm15520 mec-4(u253)* double mutant (b). In these and other panels, each red trace represents the average percentage change in R/R_0; gray shading indicates SEM of the mean response. Triangle indicates application of the harsh touch stimulus. Panel a represents the averaged response of 13 *mec-4(u253*) animals; panel b represents the response of 13 *mec-10(tm1552) mec-4(u253)* animals. **c. *mec-10* functions in the body touch neurons to promote ALM harsh touch response.** Shown is the averaged response of 17 *mec-10(tm1552) mec-4(u253); pmec-4::mec-10(+)* animals, in which *mec-10* is specifically rescued in the body touch neurons. Similar results were seen when the PVD neurons were eliminated by laser ablation (Supplemental Figure 7). **d. *degt-1* is required for ALM harsh touch responses.** Shown is the averaged response of 19 *mec-4(u253); ljEx240[pmec-4::degt-1RNAi]* animals, in which *degt-1* is specifically eliminated in the ALM neurons by RNAi. Additional off-target RNAi controls are shown in Supplemental Figure 4C. **e. Scatter plot of peak calcium responses for each genotype.** Statistical significance (*** $p < .001$;) is according to the Mann-Whitney rank sum test.

Europe PMC Funders Author Manuscripts

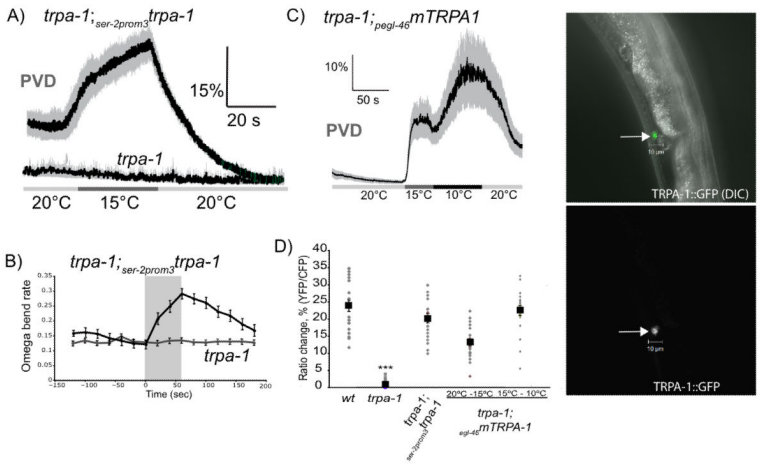

Figure 6. TRPA-1 is specifically required for cold responses in PVD

a. *trpa-1* is required for PVD cold response. Red trace indicates the averaged percentage change in R/R_0 of 17 *trpa-1(ok999)* animals; green trace is the response of 13 *trpa-1(ok999)); ljEx*245 *[pegl-46::trpa-1(+)]* animals in which a wild-type *trpa-1(+)* transgene cell-specifically rescues the null phenotype in PVD. Lower line indicates temperature changes during the recording; gray shading indicates SEM of the mean response. Scale bars are indicated in upper left. **b. *trpa-1* is required in PVD for cold shock avoidance behavior.** Shown are percentages of *trpa-1(ok999)* and PVD-rescued animals displaying avoidance behavior (omega turns) following acute temperature change (20-15° C). Blue boxes indicate the duration of the 15° C cold shock; error bars indicate SEM. **c. Mammalian mTRPA1 confers cold responses in PVD**. Red trace indicates the averaged response of 13 *trpa-1(ok999)); ljEx262 [pegl-46::mTRPA1]* animals. **d. Scatter plot of peak calcium responses for each genotype.** Statistical significance (*** $p < .001$) is according to the Mann-Whitney rank sum test. **e–f. Subcellular localization of a rescuing full-length TRPA-1::GFP fusion in PVD.** Fluorescence images of AQ2428 *ljEx267[pser-2prom3::trpa-1::GFP pmyo-2::GFP],* which express a rescuing full-length TRPA-1::GFP fusion protein in PVD. Panel e shows a single confocal section with DIC optics, while panel f shows a Z-stack confocal projection in darkfield. Phenotypic rescue of the *trpa-1* cold avoidance phenotype is shown in Supplemental Figure 5.

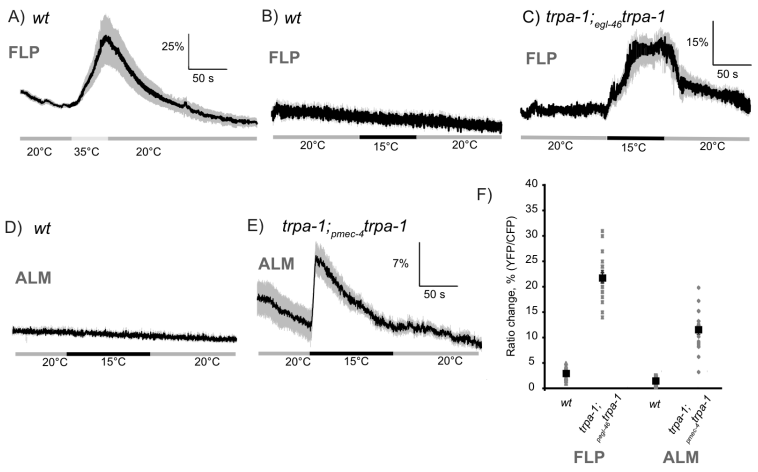

Figure 7. Heterologous expression of TRPA-1 in *C. elegans* neurons confers cold sensitivity

a. Normal response of FLP to noxious heat shock. Averaged calcium trace of wild-type FLP neurons expressing the *ljEx19* transgene. For this and other panels, the red trace represents the average percentage change in R/R_0 for 20 individual animals. Gray shading indicates SEM of the mean response, lower line indicates temperature changes during the recording. Scale bars are indicated in upper right. **b. FLP does not respond to cold shock in wild type animals.** Shown is an averaged trace of 20 wild-type *ljEx19* animals in response to 20°-15° C cold shock. **c. Animals expressing *trpa-1(+)* ectopically in FLP respond to cold shock.** Trace shows averaged response of 20 *trpa-1(ok999); ljEx246[pegl-46::trpa-1(+)]; ljEx19* animals, which express *trpa-1(+)* heterologously in FLP. **d. Wild-type ALM neurons do not respond to cold**. Shown is the averaged response of 20 *bzIs17[pmec-4::YC2.12]* animals, which express cameleon in the body touch neurons. **e. Animals expressing *trpa-1(+)* ectopically in ALM respond to cold shock.** Shown is the averaged response of 20 *trpa-1(ok999); ljEx223 [pmec-4::trpa-1(+)]; bzIs17* animals, in which *trpa-1(+)* is expressed heterologously in ALM and other the body touch neurons. **f. Scatter plot of peak calcium responses for each genotype.** Statistical significance (*** $p < .001$) is according to the Mann-Whitney rank sum test.

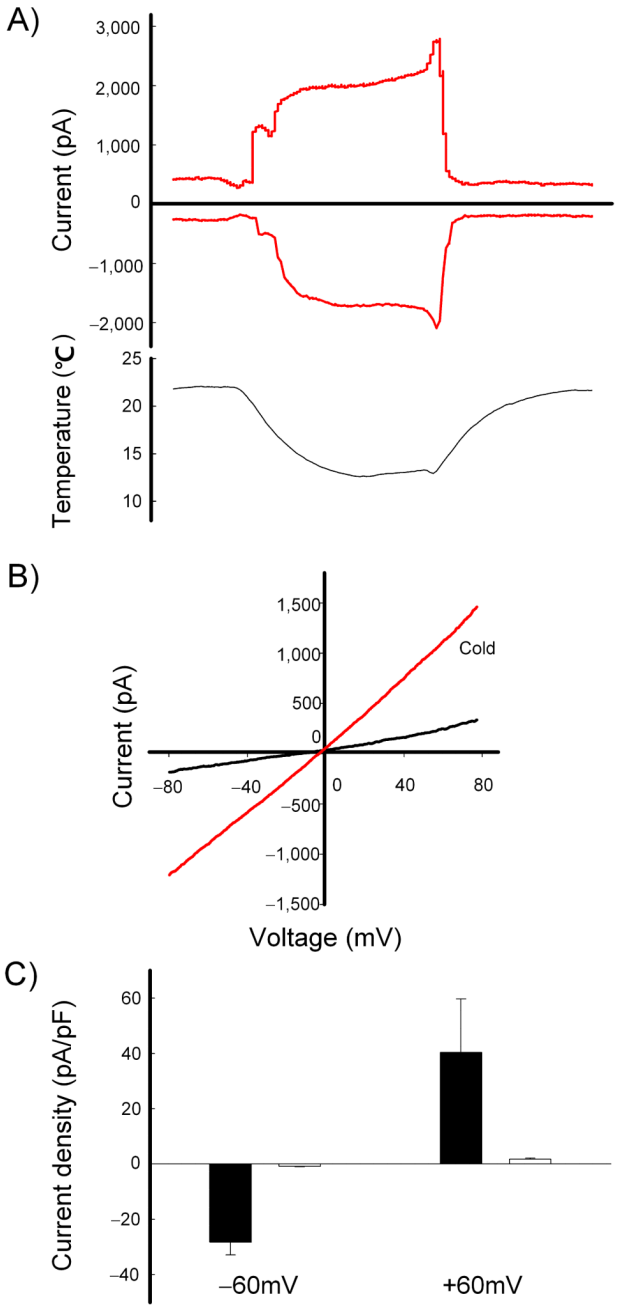

Figure 8. Cold stimuli activate TRPA-1-expressing HEK293T cells

a. TRPA-1-expressing HEK cells respond to cold in whole-cell configuration. Perfusion of the cold bath solution activates a representative TRPA-1-expressing HEK cell (n=9). Currents are shown at holding potentials of +60 and −60 mV. As previously observed in CHO cells [23], currents were also activated by pressure (Supplemental Figure 11). **b. Instantaneous current voltage relationships of the TRPA-1-expressing HEK cell are shown.** Voltages were ramped from −80 to +80 mV. Responses are shown before and during application of 15°C cold temperature in the bath. **c. Average current densities evoked by a cold temperature of 15°C.** Current densities of the cold responses of TRPA-1-

transfected (filled bars) and untransfected HEK cells (open bars) at ± 60 mV (n=9 for cold response, n=26 for no response). Error bars, ± SEM.

Europe PMC Funders Author Manuscripts